ORIGINAL ARTICLE

Dosimetric Study of Custom-made Pelvic Perspex Phantom using Single-Energy Mode (SECT) and Dual-Energy Mode (DECT) Computed Tomography

Siti Hajar Zuber[1], Nursyatina Abdul Raof[2], Rafidah Zainon[2], Abd Aziz Tajuddin[3]

[1] School of Physics, Universiti Sains Malaysia, 11800 Gelugor, Penang, Malaysia
[2] Advanced Medical and Dental Institute, Universiti Sains Malaysia, 13200 Kepala Batas, Penang, Malaysia
[3] Albukhary International University, 05200 Alor Setar, Kedah, Malaysia

ABSTRACT

Introduction: A custom-made Perspex male pelvic phantom was developed to measure and to compare absorbed, surface and effective doses obtained from Single-Energy and Dual-Energy Computed Tomography (SECT & DECT). **Methods:** A customised Perspex pelvic phantom that mimicked male Asian reference size was scanned with SECT mode at 80 kV, 100 kV, 120 kV and 140 kV. In addition, the fabricated phantom was also scanned with DECT mode at 80/140 kV. Thermoluminescence dosimeters (TLD) were used to measure the charges and doses obtained from the TLD calibration curve. The absorbed dose, surface dose and effective dose obtained from SECT and DECT were measured and compared between these two modes. **Results:** The DECT showed 55.9 % dose reduction compared to SECT at 140 kV tube voltage. It shows that DECT can be used with radiation dose sparing, and it is in good agreement with routine CTDI phantom study. The effective dose of DECT of the abdominal imaging was within the acceptable effective dose limit of AAPM Report No. 96. This study also found that the surface dose was lower than values reported in previous studies for both modes. **Conclusion:** The fabricated Perspex phantom shows a great potential to be considered as an alternative phantom for the commercially existing phantom in CT dosimetry application.

Keywords: Computed tomography, Absorbed dose, Dosimetry

Corresponding Author:
Rafidah Zainon, PhD
Email: rafidahzainon@usm.my
Tel: +604-5622554

INTRODUCTION

Computed tomography (CT) was commercially introduced in radiology in the early 1970s. It was revolutionary because it was the first fully digital imaging device. To note, more changes are occurring which expand the ability of CT, such as speed and large territory coverage (1). Recent CT development shows the ability of CT to perform dual-energy scanning to differentiate between various type of materials during imaging (2,3). In CT, radiation dose can be conveyed as volume-averaged CT dose index (CTDIvol), but it comes with certain limitations (4). The CTDI is often expressed as dose to air rather than dose to tissue and it is also measured using a standardised phantom which leads to inaccurate representation of human body (5). CTDI is often described as poor expression of dose, and more studies suggested point dose measurement as fitting and proper indicator (4). A practical option for point dose measurement is a thermoluminescence dosimeter (TLD), which can be used to assess the doses in organs at risks (OARs) in the abdomen and pelvis region during the DECT procedure.

In this study, a male pelvic phantom was fabricated to measure dose distribution in the OAR of pelvic region and its surface dose. Previously, water phantoms were used for CT dosimetry and dose descriptors measurement. Absorbed dose and effective dose are essential parameters that need to be determined accurately in dosimetry study because these values will be applied directly to the exposed entities. The depth dose profile decreases rapidly in kilovolt X-rays due to attenuation by absorbing media. The surface of the phantom is exposed to higher doses than internal body parts during diagnostic procedures involving kilovolt X-rays including in CT. Surface dose measurement can reveal the effect of high energy CT that can initiate deterministic effects such as transient erythema (6).

In this study, instead of patient being utilised to correlate to the dose absorption and calculation, a phantom material identical to human tissue was created for measuring the dose distribution in OAR of pelvic region and its surface dose. Initially, water phantom has often

been introduced and designed for CT dosimetry, and usually used to measure dose descriptors. However, it is not suitable in clinical situations and Perspex has been used as a solid homogenous phantom (7,8). Rando phantom often known as tissue equivalent phantom material in terms of its radiation absorption and scattering. It is used for dosimetry study. However, due to high cost of Rando phantom, many researchers conducted dosimetry studies using cost-effective phantom material that mimics human soft tissue (8–11). CTDI phantom was also often used in CT study. It is designed with a diameter of human head and body. CTDI phantom was made from polymethylmethacrylate (PMMA) and it has similar properties to Perspex. However, a cylindrical shape of CTDI phantom does not follow specific human body part to be contoured (12–14). Owing to the inflexible shape of existing PMMA phantom, a well-shaped phantom of human body part with placement of dosimeter is a good alternative way to measure the dose at different parts of the human body.

Reproducibility test is one of the fundamental requirements to generalise the method in phantom study. It requires harmonisation and repeatability to develop a set value or acceptable cut-off limits. It is highly desirable to include only reproducible features and variables into the method used, to be more assured of external validity across any unseen contexts. Furthermore, it is important to validate any customised phantom as reproducibility test will represent the quantitative characterisation of the phantom. According to the International Commission on Radiation Units and Measurements (ICRU) Report 44 recommendation, the uncertainties to the absorbed dose for the tissue-equivalent phantom should not be greater than 1%, otherwise, correction factor is required (15). The acceptance cut-off limit should consider the guidelines provided by ICRU for accurate data and output, while taking into consideration the characteristics of the phantom itself.

This study utilised a customised pelvic Perspex phantom and compared the absorbed dose, effective dose and surface dose of DECT mode with those of the SECT mode at 80 kV, 100 kV, 120 kV, and 140 kV in terms of dose accumulation and measurement in the OAR of the pelvic region. The potential of Perspex phantom as diagnostic phantom and its role in dosimetry study was evaluated.

MATERIALS AND METHODS

Fabrication of phantom

The CT scanned image of one centimetre slice thickness of a medium built male pelvic Perspex phantom was used to fabricate the actual size of pelvic area of Malaysian patient. It consists of organs of prostate, bladder, rectum, right and left femoral head. Perspex with density of 1.18 g·cm^{-3} was used to construct the phantom as it has the identical density to the tissue in human body (16). Thirty-one Perspex slabs were cut and constructed to represent the model of a patient's pelvic region and soft tissues. Teflon with density of 2.20 g·cm^{-3} was used to represent both femoral heads. One piece of Perspex was constructed with holes for TLDs placement and meant for the centre of the phantom.

Calibration

The customised male pelvic phantom was scanned with a Siemens Somatom Definition CT Scanner (Siemens Medical Systems; Erlangen, Germany). The fabricated phantom was shown in Fig. 1. The phantom was easy and simple to assemble and reassemble with target slice at the middle of the phantom. Thirty-one slabs of Perspex were fabricated and represented the model of male pelvic region with the organ at risk (OAR) consists of bladder, prostate, right and left femur and rectum. The scan protocol used is Abdomen-Liver protocol, Anterior Posterior projection, pitch 0.6, kernel D30f medium smooth and slice thickness of five millimetres.

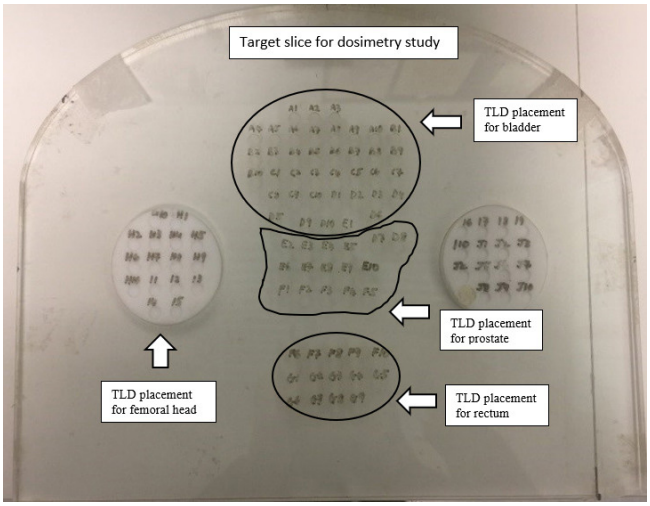

Figure 1: Contour of organ and target of the phantom for the placement of TLD for dose measurement. The slab was prepared with TLD placement to represent four regions that include right and left femoral heads, bladder, prostate and rectum.

The TLDs was calibrated using ionisation chamber with Unfors CT Detector (Raysafe; Billdal, Sweden). The dosimeter was calibrated by placing one square piece of by putting two TLD chips adjacent to the ionisation chamber, then the TLD chips was exposed to a range of doses. The conversion of signal of charge to dose from the TLDs required a calibration process. Calibration factor generated from linear regression can be established through the charge generated and doses were recorded by digital dosimeter. The response of the TLDs is energy dependent. Thus, calibration was performed at the energies used in the experiment.

In this study, the TLD responses were recorded in nano-Coulombs (nC), plotted against the ionisation chamber readings (cGy) and fit with a linear curve. The slope of

the curve was used as the conversion factor for the TLDs. The calibration curve of the TLDs for the determination coefficients were close to one. TLD was chosen over the commercially available gafchromic film because it lacks reproducibility, as the responses of film changes over time with average darkening after more than 3 months (17).

Dosimetry (Absorbed Dose, Surface Dose & Effective Dose)

High sensitivity TLDs were chosen post-calibration to evaluate organ doses and surface doses. The initial step for TLDs before and after irradiation was the annealing process to improve batch stability. The annealing process was conducted at 400 °C for one hour followed by two hours at 100 °C using the TLD Furnace (TLD Furnace LAB-01/400; Thermo Fisher Scientific, Waltham, MA, USA) to remove any residual signals in the end results. All TLDs were labelled and placed in an aluminium tray. All TLDs were tested for its consistency in dual-energy mode in the CT scanner. The standard uncertainty for each TLD measurement was ≤ 3%. All TLD readings were assumed to be accurate because the standard deviations (**σ**) for readings were in the range of 0.003–0.17. After exposure, the TLDs were treated with a pre-read heating cycle of ten minutes at 100 °C, and they were analysed using a Harshaw 3500 manual TLD reader (Thermo Electron Corporation; Reading, UK) and Window Radiation Evaluation and Management System (WinREMS) software (Saint-Gobain Crystals & Detectors; Wermelskirchen, Germany). Organ doses and surface doses were measured by TLDs during an abdominal scan of the phantom. A custom-made pelvic Perspex phantom mimicking the actual size of the pelvic area of a Malaysian patient containing the prostate, bladder, rectum, right and left femoral head was used. Dose values (cGy) were measured from the TLD readout. These values reflect the absorbed dose of the particular organ at risks in the pelvic region. Surface dose of this study was obtained directly from dose values of the TLDs placed on the pelvic Perspex phantom, and it reflects the skin dose of the pelvic region. Effective dose, E, was using the following formula in Equation 1:

$$E=\sum_T W_T H_T \text{ (mSv)} \qquad \text{(Eq. 1)}$$

where H_T is the equivalent dose in tissue or organ T and W_T is the tissue weighting factor.

RESULTS

TLD calibration curve as a function of dose

Twenty pieces of TLDs were used for calibration to produce the calibration curve by using ionisation chamber and CT phantom. Fig. 2 shows the plotted graph of dose calibration line of charge readout from TLD as a function of dose when exposed to ranges of tube current and exposure time product (mAs). Calibration factor was established by evaluation the linear regression from the charge and dose recorded from CT detector. Calibration of TLDs was performed at 80 and 140 kV as

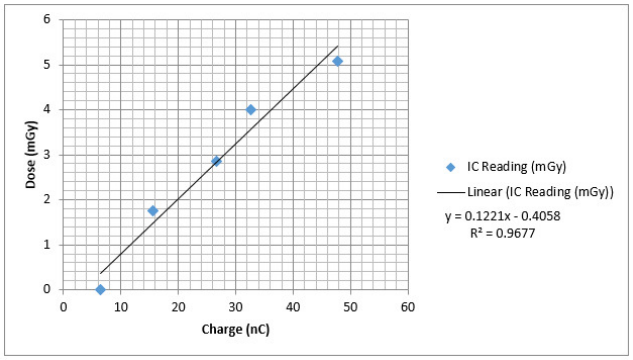

Figure 2: TLD calibration graph of dose against charge at 80 kV. Y-axis represents dose measured (mGy) and X-axis represents value of charges (nC) obtained from the calibration. IC represent ionisation chamber reading.

TLDs response is energy dependent. TLDs from both 80 kV and 140 kV tube voltage exposure yield linear dose response lines and the degree of linearity was defined by the derived coefficient of determination (r^2). The coefficients of determination (r^2) of both regression lines are high (r^2>0.9677) in this study as shown in Fig. 2. The calibration lines reveal that the TLDs used in this study had almost similar dose response. The radiation of different tube current caused different response of TLD readout to dose. TLD-100H was more prominently for high-energy dose measurement. According to previous study, the TLD-100H dosimeters have higher sensitivities than TLD-100 in terms of signals. Therefore, it has been chosen in this study (18).

Absorbed dose based on TLD measurements

Fig. 3 summarises the absorbed dose measurements of the different radiosensitive organs in this study. The absorbed dose recorded for SECT with AEC mode at 80 kV, 100 kV. It showed inconsistent increases of absorbed dose with increasing energy. However, the values were within the acceptable limit. For SECT imaging at 140

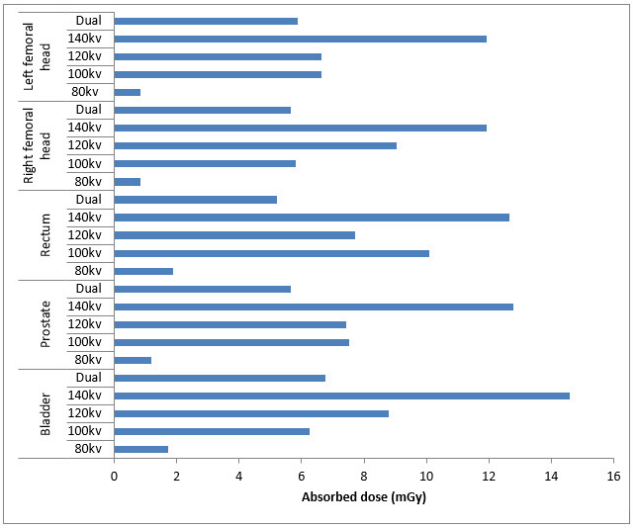

Figure 3: Comparison of absorbed doses (mGy) in high and low dose SECT and standard dose DECT. Y-axis represents the region of interest with TLD placement at different tube current (kV) and X-axis represents the absorbed dose measured (mGy).

kV, the absorbed dose reached 14.5815 mGy for the bladder and a total abdomen dose of 40.2676 mGy. In contrast, the total absorbed dose for DECT was 17.7577 mGy. The standard deviation (**σ**) is the uncertainty of dose distribution across the target on phantom. Standard deviation measures the variance of a set of numbers compared to the average or mean of the numbers. The standard uncertainty in each TLD measurement is ≤3 %.

Surface dose based on TLD measurements

The measurement of surface dose was performed by using SECT and DECT modes. The imaging parameters include pitch of 0.8, slice thickness of five millimetres and scan time of approximately six seconds. The surface doses were 1.189 mGy for 80 kV and 13.613 mGy for 140 kV for SECT and 5.253 mGy for DECT. Fig. 4 shows the surface dose (mSv) for all the protocols.

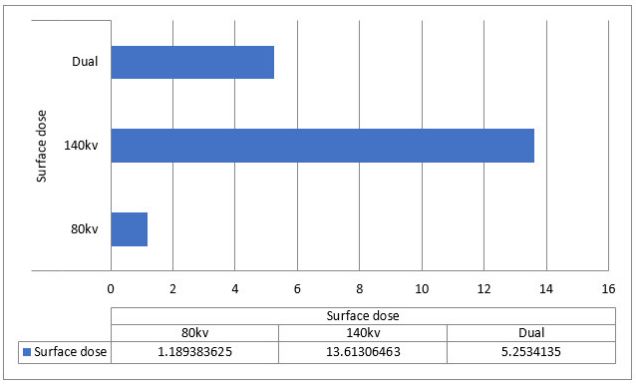

Figure 4: Comparison of surface doses (mGy) using high and low dose SECT and standard dose DECT. Y-axis represents the tube current (kV) used and X-axis represents the surface dose measured (mGy).

Effective dose calculated from TLD measurements

The effective doses measured with TLDs utilising tissue weighting factors (DECT) imaging were 0.2709 mSv for bladder, 0.6772 mSv for prostate, 0.0523 mSv for rectum, 0.0567 mSv for right femoral head and 0.0586 mSv for left femoral head, respectively. Fig. 5 shows the effective dose for different target using all the protocols of SECT mode at (80, 100, 120, 140) kV and DECT mode.

DISCUSSION

TLD calibration curve

The simple linear regression graph is used to predict a quantitative outcome of dose on the basis of one single predictor variable which is the charge collected. From calibration curve of TLDs, value of R2 closes to 1 has indicated a strong relationship between charge and dose measured.

Absorbed dose based on TLD measurements

Based on this study, absorbed doses recorded for single-energy mode of (80, 100, 120) kV with AEC showed inconsistent increment but within the acceptable value of between (0.0289 – 0.76) mGy with value less than

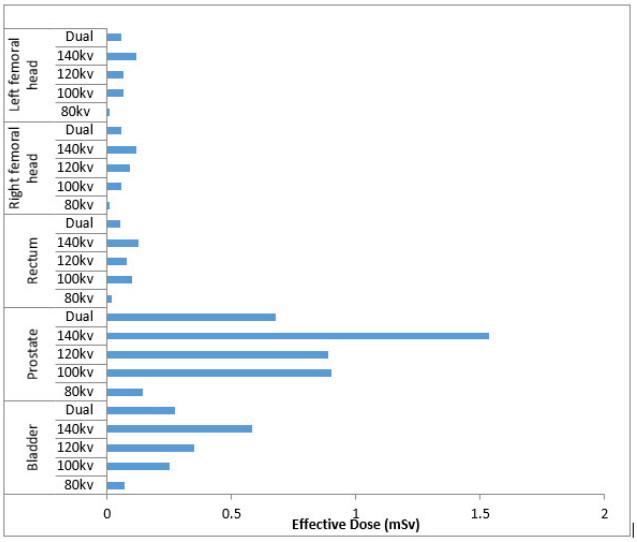

Figure 5: Comparison of effective dose (mSv) in high and low dose SECT and standard dose DECT. Y-axis represents the region of interest with TLD placement at different tube current (kV) and X-axis represents the effective dose measured (mSv).

1. The absorbed dose reached up to 14.5815 mGy for bladder in SECT imaging at 140 kV. In addition, total abdomen dose is 40.2676 mGy. On the other hand, the total absorbed dose in DECT imaging is 17.7577 mGy. DECT shows approximately 55.9% lower absorbed dose compared to SECT at 140 kV. DECT allows for routine use of lower tube voltage for abdominal imaging (20). In addition, DECT does not result in increment of radiation exposure relative to SECT, which illustrates the radiation dose sparing ability of DECT.

Surface dose based on TLD measurements

The surface dose values obtained in this study using the fabricated Perspex pelvic phantom were low compared to surface doses reported in previous studies (19). In a study using TLDs to measure surface dose for routine pelvic CT scans, Adams et al. found that mean surface dose ranged from 50 mGy to 80 mGy. For a given pitch, as the tube voltage increases the surface dose increases for SECT (19). Furthermore, large discrepancies occur between protocols that use 80 kV and those that use 140 kV tube voltage because higher tube voltage means higher radiation exposure at the surface. For DECT, the surface dose is relatively smaller in value because tube current modulation results in radiation dose sparing (20). The capability of Perspex pelvic phantom in dosimetry study was supported by relatively good outcomes of surface doses in both SECT and DECT modes.

Effective dose calculated from TLD measurements

SECT and DECT values obtained by using the fabricated Perspex pelvic phantom were within the dose estimations by ICRP Reports 103 and 60, with values differed no more than 0.4 mSv (21,22). The existing literature suggests that radiation exposure does not increase when DECT protocols are used instead of SECT in Dual-Source Computed Tomography technology. Prior studies also

showed various results in the investigation of radiation dose delivered by DECT and SECT, and the comparison between them. De Cecco et al. assessed and compared between two modes and reported a small but significant increment of DECT dose value compared with the other (23). However, the increment did not reach statistical significance of excessive radiation dose. Another study reported that there were similar trends in radiation dose between abdominal scanning between both modes while further research by another author reported that DECT mode can be executed without radiation dose penalty. (24–26).

The results of effective dose from DECT when compared with typical effective dose values provided by AAPM Report No.96, showed that the values obtained (5.25 mSv) were within the effective dose value of an abdomen and pelvis CT (8 – 14 mSv). The results revealed no apparent deviation from the values by AAPM, indicating close similarity between Perspex phantom and existing CTDI phantom. The fabricated Perspex pelvic phantom shows a great potential in replacing the CTDI phantom commonly used in dosimetry study.

The most prudent approach of estimating doses to patients in CT examination is to measure organ doses in a substitute phantom (27). Thus, the result from this study may be reliable to estimate the measure of risk although it may still be a broad assumption. The limitation of the effective dose calculation in this study is no comparison has been made with the computational method like Monte Carlo calculation. This method requires computation of repeated random sampling and statistical analysis, which cannot be obtained in the present study.

CONCLUSION

It is essential to account for the dosimetry study in the validation of newly developed phantom for medical physics application. DECT and SECT modes were carried out by employing the fabricated Perspex pelvic phantom and the results demonstrate DECT as effective at lower radiation doses compared to SECT, therefore the fabricated phantom has the potential to be used as an alternative to the conventional CTDI phantom. This finding is vital in the effort to reduce increment in patient dose due to simultaneous exposure to similar scanning volume with DECT.

ACKNOWLEDGEMENTS

The authors would like to thank the School of Physics, Universiti Sains Malaysia and Advanced Medical and Dental Institute, Universiti Sains Malaysia for the technical assistance and support during this study.

REFERENCES

1. Smyth JM, Sutton DG, Houston JG. Evaluation of the quality of CT-like images obtained using a commercial flat panel detector system. Biomed Imaging Interv J. 2006;2(4).
2. MA Hurrell, APH Butler, NJ Cook, PH Butler, JP Ronaldson, R Zainon. Spectral Hounsfield units: a new radiological concept. European Radiology. 2012. 22 (5), 1008-1013.
3. Brown CL, Hartman RP, Dzyubak OP, Takahashi N, Kawashima A, McCollough CH, et al. Dual-energy CT iodine overlay technique for characterization of renal masses as cyst or solid: a phantom feasibility study. Eur Radiol. 2009;19(5):1289.
4. Bauhs JA, Vrieze TJ, Primak AN, Bruesewitz MR, McCollough CH. CT dosimetry: comparison of measurement techniques and devices. Radiographics. 2008;28(1):245–53.
5. McCollough CH, Leng S, Yu L, Cody DD, Boone JM, McNitt-Gray MF. CT dose index and patient dose: they are not the same thing. Radiology. 2011;259(2):311–6.
6. Takegami K, Hayashi H, Yamada K, Mihara Y, Kimoto N, Kanazawa Y, et al. Entrance surface dose measurements using a small OSL dosimeter with a computed tomography scanner having 320 rows of detectors. Radiol Phys Technol. 2017;10(1):49–59.
7. Khan F, Stathakis S. The Physics of Radiation Therapy. Med Phys. 2010 Mar 1;37:1374–5.
8. Ade N, van Eeden D, du plessis F. Characterization of Nylon-12 as a water-equivalent solid phantom material for dosimetric measurements in therapeutic photon and electron beams. Appl Radiat Isot. 2019 Oct 1;155:108919.
9. Yusof MFM, Hamid PNKA, Tajuddin AA, Abdullah R, Hashim R, Bauk S, et al. Characterization and attenuation study on tannin-added Rhizophora spp. particleboard at high energy photon and electron. In: AIP Conference Proceedings. AIP Publishing; 2017. p. 40002.
10. Marashdeh MWM. Fabrication, Characterization and Dosimetric Evaluation of Rhizophora Spp. Binderless Particleboard Phantom for the Mammography and Diagnostic X-rays. Universiti Sains Malaysia; 2013.
11. Zuber SH, Hashikin NAA, Mohd Yusof MF, Hashim R. Physical and Mechanical Properties of Soy-lignin Bonded Rhizophora spp. Particleboard as a Tissue-equivalent Phantom Material. Bioresour Vol 15, No 3 [Internet]. 2020; Available from: https://ojs.cnr.ncsu.edu/index.php/BioRes/article/view/BioRes_15_3_5558_Zuber_Soy_Lignin_Bonded
12. Sharifian S, Shahbazi GD. Dose Assessment in multidetector computed tomography (CT) of polymethylmethacrylate (PMMA) phantom using

American Association of Physicists in Medicine-Task Group Report No. 111 (AAPM-TG111). 2017;
13. Ruan C, Yukihara EG, Clouse WJ, Gasparian PBR, Ahmad S. Determination of multislice computed tomography dose index (CTDI) using optically stimulated luminescence technology. Med Phys. 2010;37(7Part1):3560–8.
14. Abuhaimed A, Martin CJ, Sankaralingam M, Gentle DJ, McJury M. An assessment of the efficiency of methods for measurement of the computed tomography dose index (CTDI) for cone beam (CBCT) dosimetry by Monte Carlo simulation. Phys Med Biol. 2014;59(21):6307.
15. White DR, Buckland-Wright JC, Griffith R V, Rothenberg LN, Showwalter CK, Williams G, et al. Report 48. J Int Comm Radiat Units Meas. 1992;(1):NP-NP.
16. Radaideh KM. A custom made phantom for dosimetric audit and quality assurance of three-dimensional conformal radiotherapy. J Sains Nukl Malaysia. 2017;24(1):48–58.
17. Sim GS, Wong JHD, Ng KH. The use of radiochromic EBT2 film for the quality assurance and dosimetric verification of 3D conformal radiotherapy using Microtek ScanMaker 9800XL flatbed scanner. J Appl Clin Med Phys. 2013;14(4):85–95.
18. Sina S, Karimipoorfard M, Lotfalizadeh F, Sadeghi M, Zamani E, Zehtabian M, et al. Comparison of the response of TLD-100, and TLD-100H dosimeters in diagnostic radiology. 2014.
19. Adams EJ, Brettle DS, Jones AP, Hounsell AR, Mott DJ. Estimation of fetal and effective dose for CT examinations. Br J Radiol. 1997;70(831):272–8.
20. Kalra MK, Maher MM, Toth TL, Schmidt B, Westerman BL, Morgan HT, et al. Techniques and applications of automatic tube current modulation for CT. Radiology. 2004;233(3):649–57.
21. Wrixon AD. New ICRP recommendations. J Radiol Prot. 2008 Jun;28(2):161–8.
22. Paul J, Banckwitz R, Krauss B, Vogl TJ, Maentele W, Bauer RW. Estimation and comparison of effective dose (E) in standard chest CT by organ dose measurements and dose-length-product methods and assessment of the influence of CT tube potential (energy dependency) on effective dose in a dual-source CT. Eur J Radiol. 2012;81(4):e507–12.
23. De Cecco CN, Darnell A, Macнas N, Ayuso JR, Rodrнguez S, Rimola J, et al. Second-generation dual-energy computed tomography of the abdomen: radiation dose comparison with 64-and 128-row single-energy acquisition. J Comput Assist Tomogr. 2013;37(4):543–6.
24. Purysko AS, Primak AN, Baker ME, Obuchowski NA, Remer EM, John B, et al. Comparison of radiation dose and image quality from single-energy and dual-energy CT examinations in the same patients screened for hepatocellular carcinoma. Clin Radiol. 2014;69(12):e538–44.
25. Subhas N, Freire M, Primak AN, Polster JM, Recht MP, Davros WJ, et al. CT arthrography: in vitro evaluation of single and dual energy for optimization of technique. Skeletal Radiol. 2010 Oct;39(10):1025–31.
26. Wichmann JL, Hardie AD, Schoepf UJ, Felmly LM, Perry JD, Varga-Szemes A, et al. Single-and dual-energy CT of the abdomen: comparison of radiation dose and image quality of 2nd and 3rd generation dual-source CT. Eur Radiol. 2017;27(2):642–50.
27. McCollough CH, Christner JA, Kofler JM. How effective is effective dose as a predictor of radiation risk? Am J Roentgenol. 2010;194(4):890–6.